From Flies to Humans: Conserved Roles of CEBPZ, NOC2L, and NOC3L in rRNA Processing and Tumorigenesis

Guglielmo Rambaldelli [3], Valeria Manara [1], Andrea Vutera Cuda [1], Giovanni Bertalot [1,5,6], Marianna Penzo [3,4] and Paola Bellosta [1,2,#]

1 Department of Cellular, Computational and Integrative Biology (CIBIO), University of Trento, Via Sommarive 9, 38123 Trento, Italy
2 Department of Medicine NYU Langone School of Medicine, 550 First Avenue, 10016, NY, USA
3 Department of Medical and Surgical Sciences, University of Bologna, Via Massarenti 9, 40138 Bologna, Italy
4 IRCCS Azienda Ospedaliero-Universitaria di Bologna, 40138 Bologna, Italy
5 Unità Operativa Multizonale di Anatomia Patologica, APSS, Trento, Italy
6 CISMed, University of Trento, Via Santa Maria Maddalena 1, 38122

corresponding author: paola.bellosta@unitn.it

Abstract

NOC1, NOC2, and NOC3 are conserved nucleolar proteins essential for regulating ribosomal RNA (rRNA) maturation, a process critical for cellular homeostasis. NOC1, in *Drosophila* and yeast, enhances nucleolar activity to sustain rRNA processing, whereas its depletion leads to impaired polysome formation, reduced protein synthesis, and apoptosis. These genes have vertebrate homologs called CEBPZ, NOC2L, and NOC3l. In this study, we demonstrated that the RNA-regulatory functions of CEBPZ are conserved in vertebrates, and we showed that CEBPZ leads to the accumulation of 45S-pre rRNA, with consequent reduction in protein synthesis. Gene Ontology and bioinformatic analyses of CEBPZ, NOC2L, and NOC3L in tumors highlight a significant correlation between their reduction and the processes that regulate rRNA and 60S ribosomal maturation. Comparative analysis of their expression in tumor databases revealed that CEBPZ, NOC2L, and NOC3L exhibit contrasting expression patterns across tumor types. This dual role suggests that their overexpression promotes tumor growth, whereas reduced expression may exert tumor-suppressive effects, uncovering unexpected regulatory functions exerted by these proteins in cancer.

Keywords:
NOC1, NOC2, NOC3, CEBPZ, NOC2L, NOC3L, tumor bioinformatics, Drosophila, rRNA processing.

Introduction

Ribosome biogenesis is a highly regulated cellular mechanism that requires specific nucleolar proteins to correctly process ribosomal RNA (rRNA) necessary for ribosome maturation[1]. Disruptions in this process may lead to aberrant ribogenesis and promote tumor initiation [2-4]. The evolutionarily conserved Nucleolar Complex Proteins 1, 2, and 3 (NOC1, NOC2, and NOC3) are members of a large family of nucleolar proteins that are essential for the control of growth and viability in *S. cerevisiae* and *Arabidopsis* [5, 6 7]. NOCs were first characterized for their ability to form functional NOC1/2 and NOC2/3 heterodimers that are crucial for rRNA processing and transport during the processing of the 60S ribosomal subunit [6]. Recent studies have demonstrated that NOC1, NOC2, and NOC3 are essential for regulating RNA topology and facilitating ribosomal protein incorporation into ribosomes [3, 8-10]. NOC proteins are conserved in *Drosophila*, and we have demonstrated that their reduction leads to organ growth defects, resulting in animal lethality [11]. Specifically, we found that NOC1 is crucial for proper rRNA processing and its reduction disrupts polysome assembly and protein synthesis. Additionally, Mass Spectrometry analysis of the NOC1 interactome identified several nucleolar proteins [12], including NOC2 and NOC3, suggesting that NOC1-NOC2 and NOC2-NOC3 heterodimers also form in flies.

In vertebrates, knockout of *CEBPZ/NOC1, NOC2L, or NOC3L* results in mouse embryonic lethality[13]. Additionally, data from DepMap, a portal that explores genetic dependencies and vulnerabilities in cancer, and data from allele-specific analysis from TGCA collection genes showed that their expression is essential for tumor growth [14].

CEBPZ (ID10153) belongs to the C/EBP (CCAAT protein) family of transcription factors [15]. Known for its role as a DNA-binding transcriptional activator of heat shock protein 70, CEBPZ's function of CEBPZ in vertebrates remains largely unexplored. CEBPZ mutations have been identified in tumors of patients with acute myeloid leukemia (AML) [16]. *CEBPZ* Missense mutations in CEBPZ have been found in hereditary non-polyposis gastric cancers [17]. Its overexpression is observed in esophageal squamous carcinoma [17, 18] and is necessary to maintain m6A modifications in myeloid leukemia cells [19].

NOC2L, or NIR (Inactivator of histone acetylases), is a nucleolar histone acetyltransferase inhibitor that represses the transcription of cell-cycle genes [20]. Elevated NIR levels serve as a marker for malignancy in colorectal cancer with poor disease outcomes [20], whereas conditional knockout mice exhibit increased p53 levels, apoptosis, and bone marrow defects

[21]. Interestingly, silencing of NOC2L/NIR results in pre-rRNA accumulation and increases in p53 levels [22], and studies in mice have shown that depletion of NOC2L in LOVO tumor cells inhibits their growth in vivo [20], supporting its essential role in tumor growth.
NOC3L or Fad24 (Factor for adipocyte differentiation-24), also located in the nucleolar, is required for the proliferation of adipocyte differentiation of NIH-3T3-L1 cells [23]. In tumors, while its overexpression is linked to colorectal and gastric carcinomas, its reduction suppresses the in vitro growth of gastric cancer cells [24], suggesting a similar behavior to that reported for NOC2L in LOVO cells [20]. NOC3L is also highly expressed in stomach and pancreatic cancer. Notably, in zebrafish, the reduction of NOC3L/Fad24 significantly affects the development of hematopoietic cells [25], mirroring our data on CEBPZ reduction in zebrafish (unpublished data), suggesting a role for these proteins in the differentiation of hematopoietic cells. Furthermore, NOC3L was found to be part of the Preinitiation Complex (PIC) and necessary for DNA replication in yeast and human cells, highlighting its function in RNA transcription [26].

Here, using a multidisciplinary approach, we highlight a novel conserved role for these nucleolar proteins in ribosomal biogenesis. In *Drosophila*, NOC1, NOC2, and NOC3 are essential for rRNA processing and maturation. We propose a similar mechanism in humans, in which these three proteins work collaboratively to regulate rRNA processing and maturation. Loss or reduction in the expression of any of these genes dysregulates rRNA production, leading to impaired ribosome biogenesis and cell death. In contrast, elevated expression is associated with aggressive tumor phenotypes and poor clinical outcomes. This highlights their potential as targeting pathways to disrupt ribosome assembly to inhibit cancer growth or as biomarkers for risk assessment and survival prediction in tumorigenesis.

Results:

1. NOC proteins control rRNA processing in flies and human cells.

Ubiquitous reduction of NOC1, NOC2, or NOC3 in *Drosophila* impairs animal development, with NOC1 reduction affecting protein synthesis and inducing apoptosis [11]. Here, we show that this effect is common for all three NOCs, as reduction of either NOC1, NOC2, or NOC3 affects the correct maturation of rRNAs, as shown by the accumulation of ITS1 pre-rRNA forms (Figure 1A) and by reduction of the mature 18S ribosomal form (Figure 1B).
Furthermore, reducing the human homolog CEBPZ in HEK293T cells resulted in the accumulation of 45S pre-RNA (Figure 1C) and a significant reduction in protein synthesis, as shown by the SUnSET assay (Figure 1D-F). These data recapitulate the observations in *Drosophila* [11] and corroborate our hypothesis of an evolutionarily conserved role of CEBPZ/NOC1 in the control of rRNA maturation.
Human NOC proteins share approximately 32 % amino acid identity with their *Drosophila* homologs (Figure 1G and Supplementary File1). Analysis to predict their 3D structures using Alphafold [27, 28] imported into ChimeraX [29, 30] revealed the presence of highly similar structures in the proteins of the two species. First, the CAAT-binding protein (CBP) domain, found in both CEBPZ and NOC1 and the NOC domains, was also shared by CEBPZ and NOC3L, and a high degree of structural homology was also predicted between NOC2L and NOC2 (Figure 1H).

Based on these conserved structural similarities of key functional domains between *Drosophila* and human proteins and the conserved functional data on their rRNA regulation, we hypothesized that CEBPZ may form heterodimers with NOC2L, which are necessary for the transport and cleavage of rRNA. At state A of the 60S subunit maturation [9], the heterodimers are included in a protein complex with PES1, BOP1, FTSJ3, and WDR1, all associated with the 60S ribosome subunit, which we found to be coregulated in our analysis for CEBPZ-NOC2L co-expressing genes (Table 1 and in Figure 1I). In the second step, CEBPZ detaches NOC2L, allowing NOC3L to bind and heterodimerize with NOC2L in a new complex necessary at state C of 60S ribosomal maturation [9]. In addition to FTSJ3 and PES1, this complex contains NIP7 and DIS3, which were found to be coregulated with NOC2L-NOC3L in our expression analysis (Table 1 and in Figure 1J).

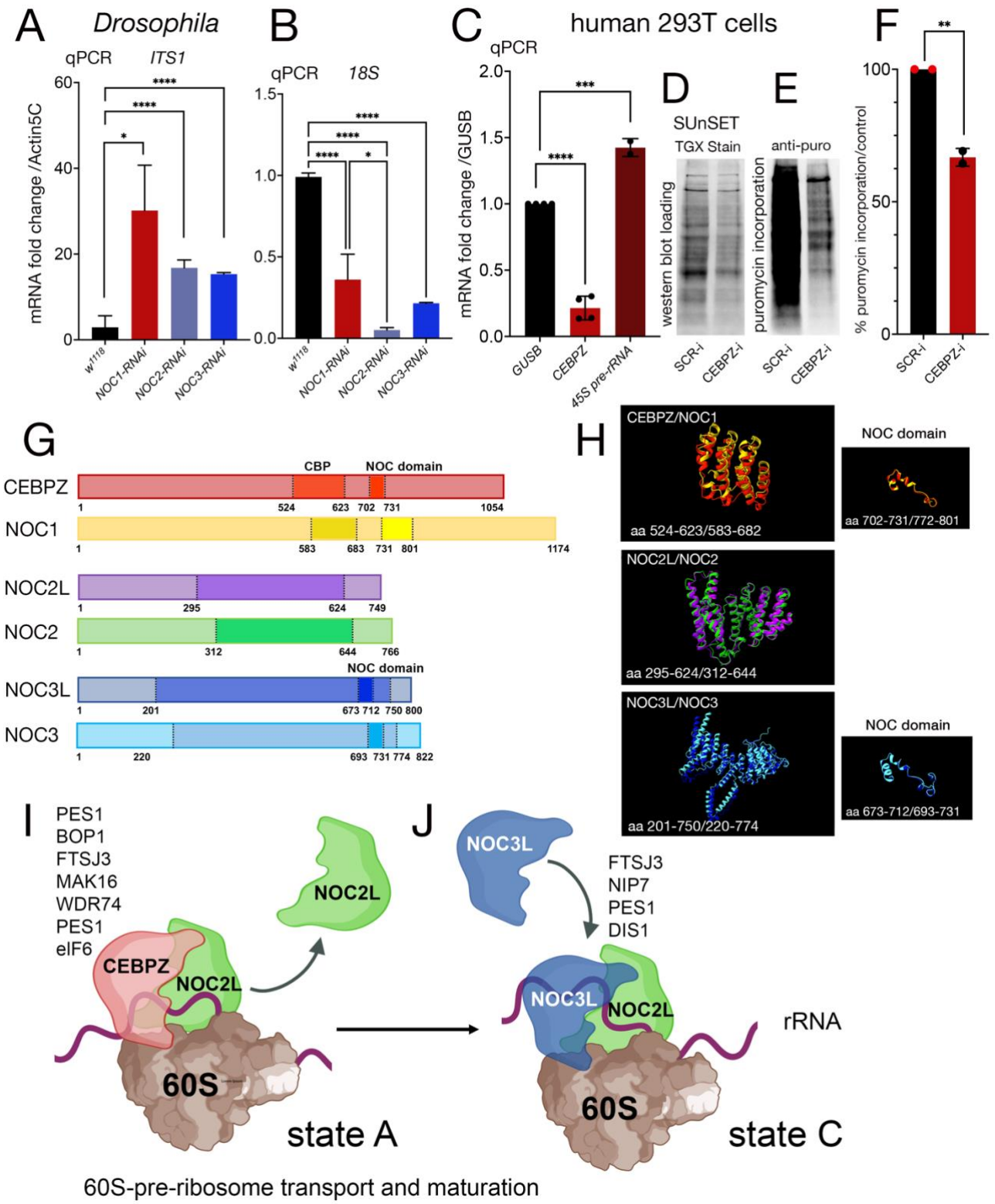

Figure 1: (A-F) Reduction of NOCs and CEBPZ induces rRNA accumulation and reduces protein synthesis. (A-B) qRT-PCRs from *Drosophila* whole larvae with ubiquitous reduced *NOC1, NOC2,* or *NOC3* showing an accumulation of pre-rRNAs, analyzed using the ITS1 (internal transcribed spacers) (A) and a reduction of rRNA18S expression (B). The level of *NOC1, NOC2,* or *NOC3-mRNAs* is calculated over control w^{1118} animals. (C) qRT-PCRs from HEK 293FT human cells where CEBPZ expression was silenced using siRNA, showing an accumulation of pre-rRNAs 45S. Data are expressed as fold increase relative to control *Actin5C* for A and B, and *Beta glucuronidase*

(GUSB) for C and presented as mean ± s.d. for at least three independent experiments **p*<0.05; ***p*<0.01; ****p*<0.001 (one-way ANOVA with Tukey multi-comparisons test). (D-E) SUnSET western blot analysis in lysates from HEK 293FT cells transfected with a scramble siRNA (SCR-i) or for siCEBPZ (CEBPZ-i) treated with 1µg/ml of puromycin for 10 minutes and lysed after 50 minutes of chase. Total proteins were extracted using RIPA buffer and resolved by 10% SDS-PAGE. (D) shows total protein loading using stain-free technologies (TGX Stain-Free Fastcast). (E) shows the relative changes in protein synthesis using anti-puromycin antibodies in cells treated with SCR-i, or CEBPZ-i. (F) A graph representing the quantification of the relative change in the rate of puromycin incorporation between SCR-i and CEBPZ-i data was analyzed using two independent experiments. (G) **Schematic representation of *Drosophila* and humans NOC1/CEBPZ, NOC2/NOC2L, and NOC3/NOC3L proteins.** CEBPZ contains a CBP domain (CCAAT binding domain in dark RED) that shares 32% aminoacid-sequence identity with *Drosophila* NOC1; and a conserved NOC domain (in dark RED). This domain is also present in NOC3L and NOC3 (highlighted in dark BLUE). NOC2 shares an overall 36% of amino acid identity between *Drosophila,* and human NOC2L, with the highest homology (48%) represented with a box; see also Supplementary File 1. **(H) The predicted structural homology of the CBP and NOC domains between CEBPZ/NOC1, NOC2L/NOC2, and NOC3L/NOC3** was obtained by a simulation using the AlphaFold and ChimeraX analysis. **(I-J) Schematic representation of the CEBPZ-NOC2L and NOC2L-NOC3L heterodimers during 60S ribosomal transport and maturation**. In this schematic draw, key proteins identified through the analysis of DepMap are highlighted for their positive correlation with the expression of NOC proteins (reported in Table 1). Their presence in the complexes is illustrated based on the stages of the 60S ribosome subunit maturation (from A to C) as outlined in the literature [1, 10]. Figure 1I-J was realized using Biorender, license EY27N2G66G.

2. Gene Ontology analysis links CEBPZ, NOC2L, and NOC3L depletion to rRNA processing and ribosome biogenesis in tumor cells.

To explore the functional significance of CEBPZ, NOC2L, and NOC3L in cancer, we analyzed data from the Cancer Dependency Portal (https://depmap.org/portal/), which utilizes CRISPR screening to identify genes that are critical for tumor growth.

Starting from the CRISPR knockdown data from DepMap, we extracted and performed our analysis on the top hundred co-expressed genes for each of the three genes of interest (Supplementary File 2), and then selected the shared co-expressed genes between the three and performed GO enrichment analysis. We then examined coregulated pathways to identify the functional implications of our genes and the possible contributions of individual heterodimers and the assembled complex.

GO network visualization (Figure 2A) highlights interconnected biological processes, including ribosome biogenesis, RNA processing, and rRNA maturation. This network underscores the close relationship between these processes, suggesting that disruptions in

components such as CEBPZ, NOC2L, or NOC3L can significantly impact ribosomal function and rRNA processing. GO enrichment analysis of genes common to all three sets also revealed a strong presence of functions associated with ribosome biogenesis, particularly rRNA processing (Figure 2B-D).

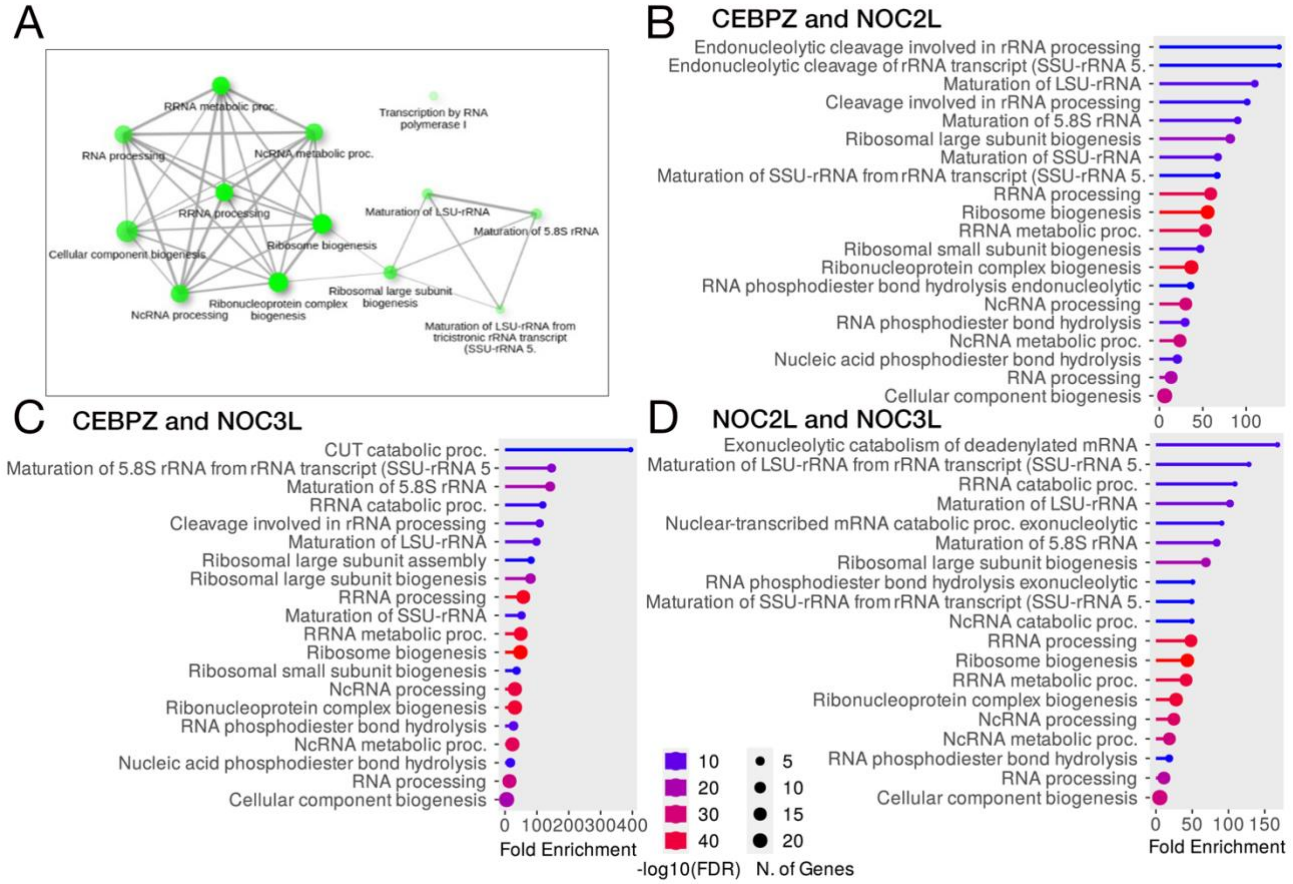

Figure 2. GO enrichment of the shared co-regulated genes between CEBPZ, NOC2L, and NOC3L. (A) Brighter nodes are more significantly enriched gene sets. Bigger nodes represent larger gene sets. Thicker edges represent a higher number of genes shared between the two sets. (B-D) **GO enrichment (Biological Processes) of the shared co-regulated genes between two target genes.** The results are ordered based on the Fold Enrichment; the circle size represents the number of genes in the pathway, the color of the bars the -log10(FRD), and the length of the bar the enrichment.

DepMap and GO analyses revealed a significant enrichment of genes associated with ribosome biogenesis and rRNA processing when CEBPZ or NOC2L expression was reduced (Table 1 and Figure 2B). It is plausible that decreasing the expression levels of CEBPZ or NOC2L disrupts the formation of CEBPZ-NOC2L heterodimers, leading to rRNA accumulation and affecting the maturation of the ribosomal 60S subunit. Additionally, although to a lesser extent, we found that reduction of the NOC2L-NOC3L interaction affects RNA processing and ribosome biogenesis (Figure 2C), reinforcing our hypothesis that both

pairs play a role in regulating rRNA maturation, and impairment of either heterodimer disrupts rRNA maturation, leading to its accumulation (Figure 1C). Moreover, these data also revealed that when CEBPZ levels were reduced, NOC2L expression also diminished, and the reverse was true (see Supplementary File 2), suggesting the possibility of co-regulation mechanisms between the two proteins that may be necessary for the proper stoichiometric expression and formation of heterodimers.

gene	Positively correlating with the downregulation of CEBPZ and NOC2L
WDR36	Part of the small subunit (SSU) processome, first precursor of the small eukaryotic ribosomal subunit.
WDR74	Regulatory protein of the MTREX-exosome complex involved in the synthesis of the 60S rib.subunit.
RPL13A	Associated with ribosomes but is not required for canonical ribosome function.
GRWD1	Histone binding-protein that regulates chromatin dynamics and mini chromosome maintenance.
LAS1L	Required for the synthesis of the 60S ribosomal subunit and maturation of the 28S rRNA.
POLR1E	Component of RNA polymerase I polymerase which synthesizes ribosomal RNA precursor.
TBL3	Part of the small subunit (SSU) processome, first precursor of the small eukaryotic ribosomal subunit.
PWP1	Regulates Pol I-mediated rRNA biogenesis and, probably, Pol III-mediated transcription.
NAT10	RNA cytidine acetyltransferase catalyzes the formation of N_4-acetylcytidine modification on18S and rRNA.
UTP4	Involved in nucleolar processing of pre-18S ribosomal RNA. Part of the small subunit (SSU) processome.
DKC1	small nucleolar ribonucleoprotein (H/ACA snoRNP) complex, which catalyzes pseudouridylation of rRNA.
NOP16**	Involved in the biogenesis of the 60S ribosomal subunit.
RPP38	Component of ribonuclease Pcomplex that generates mature tRNA molecules by cleaving their 5'-ends.
WDR18	Component of the PELP1 complex involved in the 28S rRNA maturation and the transit of the pre-60S.
DIS3**	Putative catalytic component of the RNA exosome complex 3'->5' exoribonuclease activity.
DHX33	Implicated in nucleolar organization, stimulates RNA polymerase I transcription of the 47S precursor rRNA. Associates with ribosomal DNA (rDNA) loci where it is involved in POLR1A recruitment
PAK1IP1	Negatively regulates the PAK1 kinase.
NIP7	Required for 34S pre-rRNA processing and 60S ribosome assembly.
ISG20L2	3'-> 5'-exoribonuclease involved in ribosome biogenesis in the processing of the 12S pre-rRNA.
NOL9	Involved in rRNA processing, required for the processing of the 32S precursor into 5.8S and 28S rRNAs.
PPAN	A chimeric transcript, characterized by the first third of PPAN exon 12 joined to P2RY11 exon 2.
POLR1G	Component of RNA polymerase I (Pol I) which synthesizes ribosomal RNA precursors.
MYBBP1A	May activate or repress transcription via interactions with sequence specific DNA-binding proteins.
NOC4L	Nucleolar complex-associated protein 4-like protein.
EIF6	Binds to the 60S subunit and prevents its association with the 40S to form the 80S initiation complex.
POP5	Component of ribonuclease P, that generates mature tRNA molecules by cleaving their 5'-ends.
URB2	Essential for hematopietic stem cell development through the regulation of p53/TP53 pathway.
TIMM50**	Component of the TIM23 complex, that mediates the translocation of transit peptide-containing proteins.
UTP20	Part of the small subunit (SSU) processome, first precursor of the small eukaryotic ribosomal subunit.
BOP1	Component of the PeBoW complex, which is required for maturation of 28S and 5.8S ribosomal RNAs.
UTP23	Involved in rRNA-processing and ribosome biogenesis.
MAK16	Important for the maturation of LSU-rRNA and 5.8S rRNA
DIMT1	Demethylates two adjacent adenosines in the loop of a conserved hairpin near the 3'-end of 18S rRNA in the 40S particle. Involved in the pre-rRNA processing leading to small-subunit rRNA.
PDCD11	Essential for the generation of mature 18S rRNA, necessary for cleavages at sites A0, 1 and 2 of the 47S.
DDX21	RNA helicase acts as a sensor of the transcriptional status of RNA polymerase (Pol) I and II: promotes ribosomal RNA (rRNA) processing and transcription from polymerase II (Pol II)
TAF1C	Component of the transcription factor SL1/TIF-IB complex, which is involved in the assembly of the PIC (pre-initiation complex) during RNA polymerase I-dependent transcription.
FTSJ3	RNA 2'-O-methyltransferase involved in the 34S pre-rRNA to 18S rRNA and in 40S ribosomal formation.

IMP4	Component of the 60-80S U3 small nucleolar ribonucleoprotein (U3 snoRNP).
PWP2	Part of the small subunit (SSU) processome, first precursor of the small eukaryotic ribosomal subunit.
DDX51	ATP-binding RNA helicase involved in the biogenesis of 60S subunits.
PES1**	PeBoW complex, required for maturation of 28S and 5.8S ribosomal RNAs and formation of the 60S.
NHP2	Required for ribosome biogenesis and telomere maintenance. Part of the H/ACA small nucleolar ribonucleoprotein complex, which catalyzes pseudouridylation of rRNA.
RRP12	Required for nuclear export of both pre-40S and pre-60S subunits.
WDR75	Part of the small subunit (SSU) processome, precursor of the small eukaryotic ribosomal subunit.
RRP1*	critical role in the generation of 28S rRNA
DDX56*	Nucleolar RNA helicase that controls nucleolar integrity and RiBi
NOL12*	RNA binding protein that plays a role in RNA metabolism, the resolution of DNA stress, nucleolar organization, regulates the levels of nucleolar fibrillarin and nucleolin in pre-rRNA processing.
RPP14*	ribonucleoprotein complex that generates mature tRNA molecules.
PELP1*	Component of the PELP1 complex involved in the 28S rRNA maturation and transit of the pre-60S.

Table 1: List of the genes and their function that positively correlate with CEBPZ and NOC2L reduction in tumor cells. * Genes that positively correlate when CEBPZ and NOC3 are reduced; ** Genes that positively correlate when all three genes are reduced. For the whole list for each gene, see Supplementary File 2. Annotation of their function from UniProt (https://www.uniprot.org/) [31].

3. CEBPZ, NOC2L and NOC3L tumor expression analysis.

Dysregulation of rRNA processing is a hallmark of many cancers. Starting from the hypothesis that the three genes work together to form heterodimers that regulate rRNA processing, we analyzed how their expression changes across various tumor types. Thus, we examined CEBPZ, NOC2L, and NOC3L expression levels in TCGA data from the UALCAN cancer portal database [32, 33] (Figure 3A-C). This analysis revealed that all were significantly upregulated (red) in adrenocortical carcinoma (ACC), cholangiocarcinoma (CHOL), esophageal carcinoma (ESCA), Head and Neck squamous carcinoma (HNSC), liver hepatocellular carcinoma (LIHC), lung adenocarcinoma (LUAD), rectum adenocarcinoma (READ), stomach adenocarcinoma (STAD), Uterine Corpus Endometrial Carcinoma (UCEC), and Uveal Melanoma (UVM) tumors. In contrast, their expression was significantly reduced (green) in Kidney Chromophobe carcinoma (KICH), whereas only CEBPZ and NOC3L were significantly reduced in kidney renal clear cell carcinoma (KIRC), kidney papillary cell carcinoma (KIRP), and acute myeloid leukemia (LAML) cancers (Figure 3D).

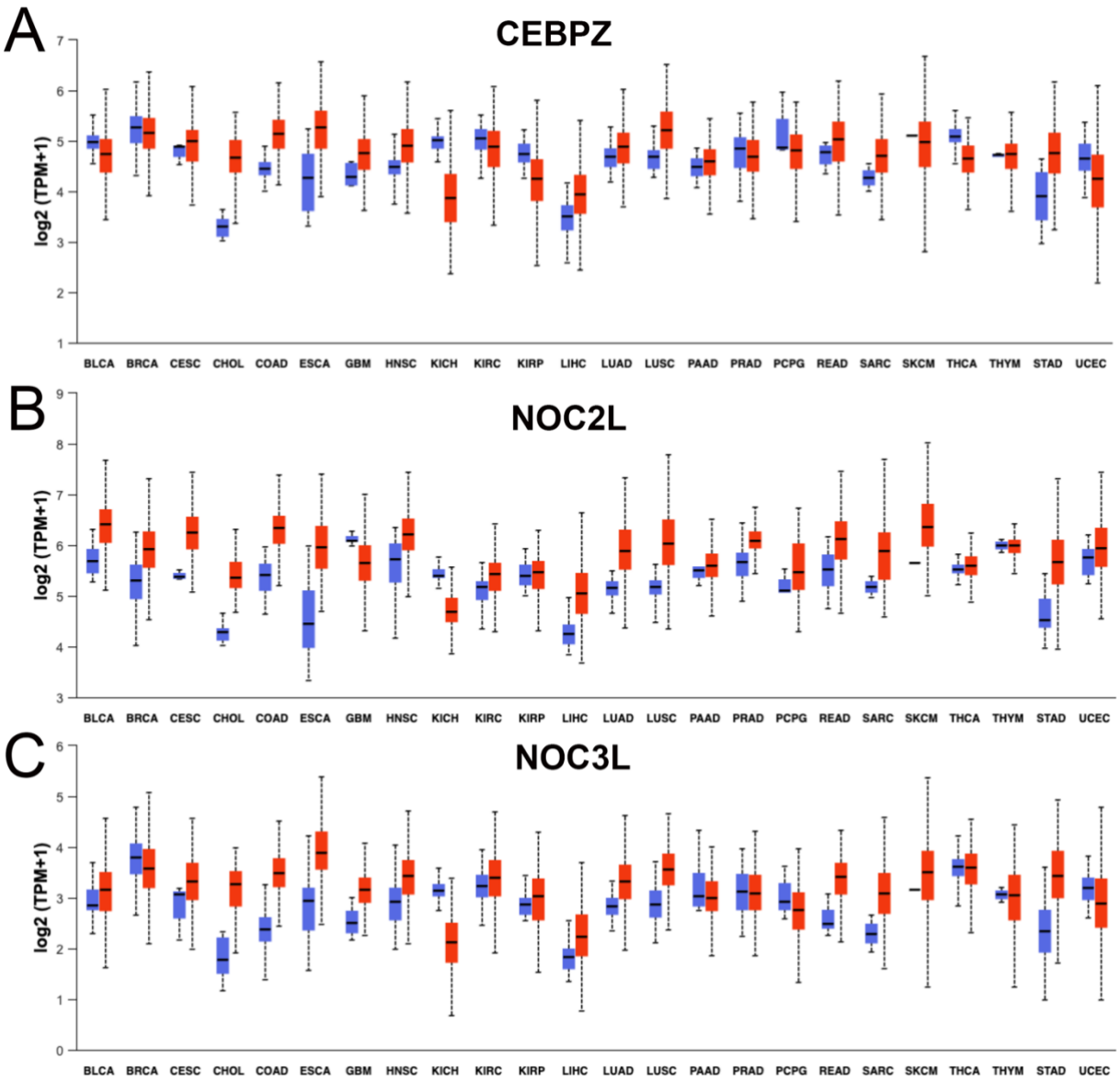

D **Expression of CEBPZ, NOC2L, and NOC3L in tumors vs. normal tissues (TCGA)**

Classification Name	TUMOR	CEBPZ	NOC2L	NOC3L
Adrenocortical carcinoma	ACC	0.00088	0.006	0.004
Cholangiocarcinoma	CHOL	< 0.0001	< 0.0001	< 0.0001
Esophagean carcinoma	ESCA	0.0003	< 0.0001	0.0004
Head and Neck squamous carcinoma	HNSC	< 0.0001	< 0.0001	< 0.0001
Kidney Chromophobe	KICH	< 0.0001	<0.0001	<0.0001
Kidney renal clear cell carcinoma	KIRC	0.003	< 0.0001	0.003
Kidney renal papillary cell carcinoma	KIRP	< 0.0001	0.1	0.003
Acute myeloid leukemia	AML	< 0.001	0.007	<0.0001
Liver hepatocellular carcinoma	LIHC	< 0.0001	< 0.0001	< 0.0001
Lung adenocarcinoma	LUAD	< 0.0001	< 0.0001	< 0.0001
Lung squamous cell carcinoma	LUSC	< 0.0001	< 0.0001	< 0.0001
Rectum adenocarcinoma	READ	0.003	0.0004	< 0.0001
Stomach adenocarcinoma	STAD	< 0.0001	< 0.0001	< 0.0001
Uterine Corpus Endometrial Carcinoma	UCEC	0.0005	< 0.0001	0.001
Uveal Melanoma	UVM	< 0.0001	< 0.0001	0.001

Figure 3: Gene expression analysis (TCGA). CEBPZ (A), NOC2L (B), and NOC3L (C) expression in tumors versus normal tissues. (D) This panel shows data from tumors (A-C) where the expression levels of CEBPZ, NOC2L, and NOC3L are significantly altered ($p < 0.05$). Red indicates overexpression, while green represents reduced expression.

To conduct a deeper analysis of CEBPZ, NOC2L, and NOC3L expression at different stages of tumor progression, we utilized data reported in the UALCAN cancer portal. This analysis revealed a significant increase in the expression of CEBPZ, NOC2L, and NOC3L in liver hepatocellular carcinomas (Figure 4A) and lung adenocarcinoma (Figure 4B). The observed upregulation correlated with the progression of tumor stages. The expression levels of LIHC in stage 4 were comparable to those in controls, possibly because of the reduced sample size for this stage. Similar upregulation was found for rectum adenocarcinoma (READ) and stomach adenocarcinoma (STAD) (not shown), suggesting that CEBPZ, NOC2L, and NOC3L overexpression may contribute to the aggressiveness of these carcinomas, probably by increasing rRNA processing and ribosome activity. In contrast, in kidney carcinomas, CEBPZ, NOC2L, and NOC3L expression levels were consistently and significantly reduced in KICH, but variable in other types of kidney cancers (Figure 4C-E).

To investigate the co-expression patterns of CEBPZ, NOC2L, and NOC3L within kidney tumors, we analyzed TCGA dataset publicly accessible through FireBrowse [34]. A Pearson correlation coefficient was calculated between the expression of the three genes (CEBPZ, NOC2L, and NOC3L) in the three kidney carcinoma subtypes (KICH, KIRC, and KIRP). This analysis showed that CEBPZ and NOC3L exhibited a strong direct correlation in all three tumors (Table 2). Meanwhile, a weak negative correlation existed between CEBPZ and the other two genes in both KIRC and KIRP. This suggests the potential distinct roles of these genes in tumor behavior and prognosis across various kidney cancers.

KICH				**KIRC**				**KIRP**			
r				r				r			
	CEBPZ	NOC2L	NOC3L		CEBPZ	NOC2L	NOC3L		CEBPZ	NOC2L	NOC3L
CEBPZ	1	-0,035481	0,7768214	CEBPZ	1	-0,263372	0,5205663	CEBPZ	1	-0,223414	0,4592963
NOC2L	-0,035481	1	0,1116638	NOC2L	-0,263372	1	-0,225758	NOC2L	-0,223414	1	-0,151207
NOC3L	0,7768214	0,1116638	1	NOC3L	0,5205663	-0,225758	1	NOC3L	0,4592963	-0,151207	1
P				*P*				*P*			
	CEBPZ	NOC2L	NOC3L		CEBPZ	NOC2L	NOC3L		CEBPZ	NOC2L	NOC3L
CEBPZ	NA	0,7384625	0	CEBPZ	NA	4,50E-11	0	CEBPZ	NA	5,10E-05	0
NOC2L	0,7384625	NA	0,2919838	NOC2L	4,50E-11	NA	1,92E-08	NOC2L	5,10E-05	NA	0,0064759
NOC3L	0	0,2919838	NA	NOC3L	0	1,92E-08	NA	NOC3L	0	0,0064759	NA

Table 2: A matrix to highlights the significant correlation between CEBPZ, NOC2L, and NOC3L expression in KICH, KIRC, and KIRP kidney carcinomas. It also shows that for each tumor type, the r (correlation coefficient) and the P value, highlighted in blue, are significant, with a correlation higher than -/+ 0.4. A higher absolute number means a stronger correlation between the samples' expression levels. (e. g. In KICH, when CEBPZ is low, also NOC3L is low) The lower part of the table shows the P-value for each correlation, highlighting the significant ones ($p<0.05$).

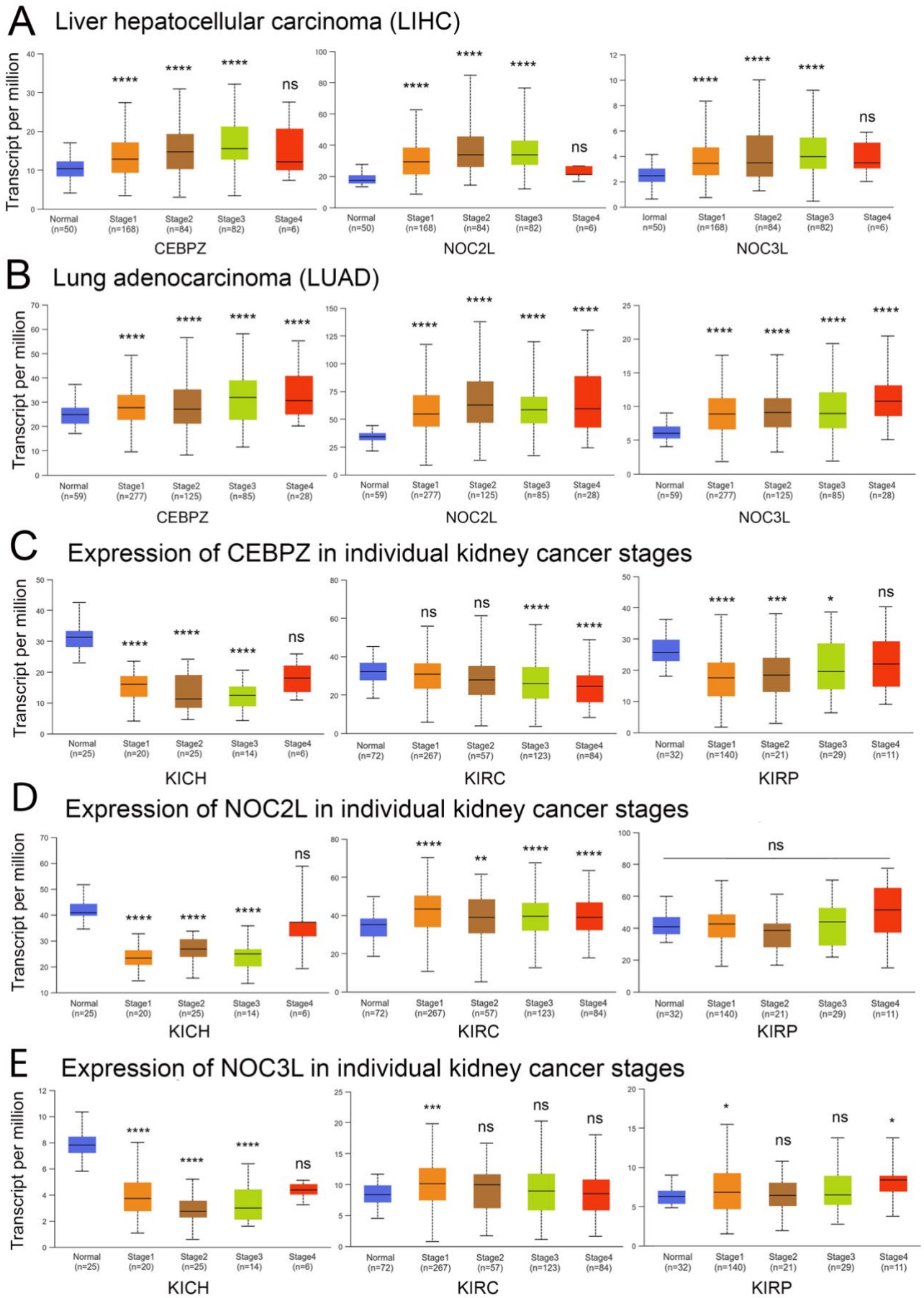
A Liver hepatocellular carcinoma (LIHC)
Transcript per million
Normal (n=50)
Stage1 (n=168)
Stage2 (n=84)
Stage3 (n=82)
Stage4 (n=6)
CEBPZ
NOC2L
NOC3L
B Lung adenocarcinoma (LUAD)
Normal (n=59)
Stage1 (n=277)
Stage2 (n=125)
Stage3 (n=85)
Stage4 (n=28)
C Expression of CEBPZ in individual kidney cancer stages
KICH
KIRC
KIRP
D Expression of NOC2L in individual kidney cancer stages
E Expression of NOC3L in individual kidney cancer stages

Figure 4: Graphs illustrating expression levels across various cancer types during tumor progression. Data from UALCAN highlights the correlation between gene expression and disease progression, demonstrating significant change in the expression of CEBPZ, NOC2L, and NOC3L with advancing disease stages. (A) Liver hepatocellular carcinoma (HCC) and (B) Lung adenocarcinoma (LUAD), (C-E) Expression of CEBPZ, NOC2L, and NOC3L in KICH, KIRC, and KIRP kidney cancers, The statistical analysis was performed by comparing the expression levels of the indicated genes in tumors at various stages to their expression levels in normal control tissue, data are from UALCAN portal[32, 33]. Statistical significance is expressed by the asterisks **** $p < 0.0001$, *** $p < 0.001$, ** $p < 0.01$, and * $p < 0.05$. ns not significative

3.2 Impact of CEBPZ, NOC2L, and NOC3L expression on patient survival.

We analyzed the correlation between the expression of CEBPZ, NOC2L, and NOC3L and patient survival to explore their potential impact on disease outcomes across tumor types. Figure 5 displays a heatmap of hazard ratios for these genes, providing a visual summary of how their expression is related to survival in various tumors.

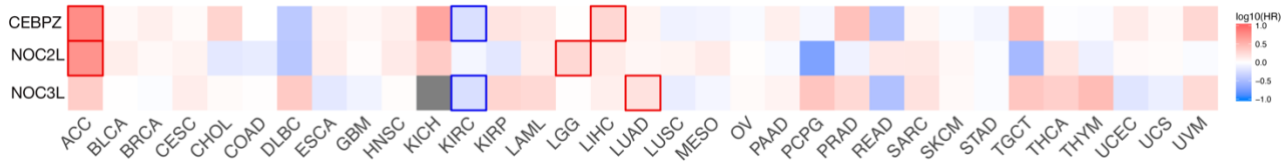

Figure 5: Hazard ratio (HR) heat map for CEBPZ (ID: ENSG00000115816.13), NOC2L (ID: ENSG00000188976.10), and NOC3L (ID: ENSG00000173145.11) in the tumors listed below. The median is selected as a threshold for separating high-expression and low-expression cohorts. The bounding boxes depict the statistically significant results ($p < 0.05$). Colors from white to red indicate an HR above 1, suggesting that high gene expression is associated with a worse prognosis. Colors from white to blue indicate an HR below 1, suggesting that high gene expression is associated with a better prognosis.

These data suggest that the expression of CEBPZ and NOC2L in adenoid cystic carcinoma (ACC) may be associated with poorer tumor prognosis. This means that as the expression levels of these genes increase, the severity or aggressiveness of cancer may also increase, potentially leading to worse patient outcomes. A similar trend was observed in brain lower-grade glioma (LGG), liver hepatocellular carcinoma (LIHC), and lung adenocarcinoma (LUAD), with different degrees of significance (Figure 5). In contrast, in kidney chromophobe carcinoma, there was an inverse correlation between CEBPZ and NOC3L expression and patient outcomes. Additionally, CEBPZ, NOC2L, and NOC3L exhibited distinct expression patterns during the progression of kidney carcinoma, with a marked decrease observed in KICH (Figure 4C-E). This reduction suggests that disrupting RNA metabolism and ribosome biogenesis by downregulating these genes may influence cellular processes that drive cancer progression in specific cell types, such as kidney cells.

Discussion:

This study revealed an evolutionarily conserved role of CEBPZ, NOC2L, and NOC3L in regulating ribosomal biogenesis. Our cross-species analysis demonstrated that these genes are critical for rRNA maturation and ribosomal activity and are essential for cellular growth and survival in *Drosophila* and human cells, underscoring their novel and conserved function in controlling RNA processing.

Our previous analysis of the NOC1 protein interactome identified NOC2 and NOC3 proteins within the NOC1-nucleolar complex [12]. Additionally, our unpublished data suggest that NOC proteins do not compensate for each other's function. These findings align with those of previous yeast studies, where NOCs were shown to be essential for life and to form NOC1-NOC2 and NOC2-NOC3 heterodimers necessary for rRNA processing [3, 6]. Based on these observations, we hypothesized that in humans, CEBPZ, NOC2L, and NOC3L may function as heterodimer complexes to control rRNA maturation, as illustrated in the model shown in Figure 2I-J.

Our TGCA and GO analyses suggest that CEBPZ, NOC2L, and NOC3L expression levels influence tumor growth by regulating rRNA maturation and ribosome production processes. Overexpression of these genes may enhance ribosome biogenesis and sustain tumor progression in liver, rectal, and lung carcinomas, and recently, CEBPZ has been found in a genetic screen as a mediator of epithelial-mesenchymal transition in lung cancer [35].
The paradox is that in kidney carcinomas and acute myeloid leukemia, these genes are downregulated, resulting in impaired ribosomal function. This could contribute to cell-specific responses and the activation of oncogenic mechanisms.

Such opposite expression patterns have already been described for other ribosome-biogenesis-related factors, such as dyskerin, rRNA pseudouridine synthase, fibrillarin, and rRNA 2'-O-methyltransferase. The activity of these two enzymes is required for correct rRNA maturation and ribosomal function [36] [37]. An impact on tumor development has been highlighted, for both, either in the case of increased or reduced expression, in different oncologic settings. On the one hand, fibrillarin upregulation has been correlated with a worse prognosis in breast cancer [38] and acute myeloid leukemia [39]; on the other hand, its reduction has been linked to a worse outcome in breast cancer [40]. Similarly, dyskerin downregulation

has been shown to favor breast cancer development [41] and has been correlated with a worse prognosis in endometrial cancer [42], while its higher expression correlates with the development of colorectal cancer [43], breast cancer [44, 45], prostate cancer [46], and others. Paradoxically, the downregulation of NOC proteins (e.g., NOC2L and NOC3L) could favor tumor growth in specific cancers, such as kidney carcinomas and acute myeloid leukemia, by impairing ribosomal function and inducing nucleolar stress, with the possibility of inducing DNA damage and the disruption of DNA repair mechanisms that favor tumor initiation [4].

In conclusion, we have identified CEBPZ, NOC2L, and NOC3L as novel regulators of rRNA processing and ribosome biogenesis. Their expression levels in tumors vary significantly depending on cellular and tissue context. High expression is observed in most tumor types and is typically associated with aggressive tumor behavior. In contrast, low expression in renal cancers, mainly KICH and AML, correlates with advanced tumor stages. These findings suggest that rRNA dysregulation influences cancer progression through distinct context-dependent mechanisms shaped by the cellular environment and tissue type. Assessing the expression of these genes in physiological tissues and specific tumor contexts could provide valuable insights into their role in ribosomal biogenesis in cancer progression and aid in the development of targeted diagnostic and prognostic biomarkers.

Material and Methods

Fly husbandry

Fly cultures and crosses were raised at 25 °C on a standard medium containing 9 g/L agar (ZN5 B and V), 75 g/L corn flour, 60 g/L white sugar, 30 g/L brewers' yeast (Fisher Scientific), 50 g/L fresh yeast, 50 mL/L molasses (Naturitas), along with nipagin, and propionic acid (Fisher). The lines used *NOC1-RNAi* (B25992), *NOC2-RNAi* (B50907), *and NOC3-RNAi* (B61872) were obtained from the Bloomington Drosophila Stock Center.

WB SUnSET assay

UAS-NOC1-RNAi was expressed ubiquitously in whole larvae using *actin-Gal4* coupled with *tubulin-Gal80* temp-sensitive allele to avoid early lethality. Crosses were maintained at 18 °C, and when larvae reached the second instar, they were switched to 30 °C for 72 h before

dissection. At least seven third-instar larvae of each genotype were dissected in Schneider's medium and then transferred to Eppendorf tubes containing complete medium with 10 % serum plus puromycin at 20 µg/ml (Invitrogen, Thermo Fisher Scientific). The samples were incubated for 40 or 60 min at room temperature, then recovered in 10 % serum/medium without puromycin for 30 min at room temperature. The inverted larvae were snap-frozen in liquid nitrogen for subsequent western blot analysis using an anti-puromycin primary antibody.

Cell culture and RNAi

HEK-293FT cells (ThermoFisher Scientific) were cultured in DMEM (Corning Inc.) supplemented with 10 % FBS, 2mM L-glutamine, 100 U/ml penicillin, and 100 µg/ml streptomycin (all from Sigma-Aldrich) and maintained at 37 °C, 5 % CO_2 in a humidified incubator. For RNA interference, cells were transfected with Lipofectamine RNAiMAX (ThermoFisher Scientific) following the manufacturer's specifications. Transfected siRNA sequences were as follows: siRNA CEBPZ_1: rCrArArArArGrUrCrArGrUrArCrUrArArArArArArArGrCAA; siRNA CEBPZ_2: rUrUrGrCrUrUrUrUrUrUrArGrUrArCrUrGrArCrUrUrGrArG; negative control: scrambled negative control DsiRNA, all from Integrated DNA Technologies). 72 hours after transfection, the cells were harvested, and total RNA was extracted.

Rna extraction and RT-PCR

RNA was extracted from Drosophila larvae or HEK 293FT human cells using the RNeasy Mini Kit (Qiagen) following the manufacturer's instructions. The isolated RNA was quantified using a Nanodrop2000. Total RNA (1000 ng of total RNA was reverse-transcribed into complementary DNA (cDNA) using SuperScript IV VILO Master Mix (Invitrogen). The obtained cDNA was used for qRT-PCR with the SYBR Green PCR Kit (Qiagen). The assays were performed on a Bio-Rad CFX96 machine and analyzed using Bio-Rad CFX Manager software. Transcript abundance was normalized using *actin5c.* The primer list was published in [11]. For human targets, primers were purchased from Integrated DNA Technologies: CEBPZ forward: TCTCATCCAAAGTAGCCAGCAT; reverse: TCTCATCCAAAGTAGCCAGCAT; 45S pre-rRNA forward: GAACGGTGGTGTGTCGTTC;

45S pre-rRNA reverse: GCGTCTCGTCTCGTCTCACT); and GUSB housekeeping expression kit was purchased from Applied Biosystems (ref 4326320E).

Statistical Analysis

Students' *t*-test analysis and analysis of variance were calculated using one-way ANOVA, and Tukey's multiple comparisons test was calculated using GraphPad-PRISM*8. p* values are indicated with asterisks *** =** $p < 0.05$, ** = $p < 0.01$, *** = $p < 0.001$, **** = $p < 0.0001$, respectively.

Correlations

TCGA data were accessed through FireBrowse (Broad Institute TCGA Genome Data Analysis Center (2016): Firehose 2016-01-28 run. Broad Institute of MIT and Harvard. doi:10.7908/C11G0KM9) and processed in-house using the r-corr function of the Hmisc package in R. (https://www.rdocumentation.org/packages/Hmisc/versions/5.1-3) [47]

Differential expression and HR heat-map

Differential expression analysis was conducted using the GEPIA2 [47] platform to compare gene expression profiles between tumor and normal samples derived from the TCGA and GTEx datasets. GEPIA2 was also used to produce a survival heat map of hazard ratio.

Gene Ontology enrichment

GO and KEGG enrichment analyses were performed using ShinyGO [48] with an FDR cutoff of 0.5. The shared coregulated genes between CEBPZ, NOC2L, and NOC3L were tested.

Co-expressed genes

Broad DepMap https://depmap.org/portal/(Project data public release 24Q4) was used to determine the genes' dependencies after CRISPR in cancer cell lines [49-51]. The Broad DepMap project reports essentiality scores using the Chronos algorithm [52]. A lower score indicates a greater probability that the gene of interest is essential in a specific cell line. A

score of 0 denotes a non-essential gene, whereas a score of -1 reflects the median for pan-essential genes.

Tumor stage expression

The expression levels of the three genes of interest have been explored through UALCAN at https://ualcan.path.uab.edu [32, 33]

Acknowledgments

We thank the Bloomington Stocks Center Stock Center (NIH P40OD018537). Department CIBIO Core Facilities is supported by the European Regional Development Fund (ERDF) 2014–2020. This article is based on work from COST Action CA21154 TRANSLACORE, supported by COST (European Cooperation in Science and Technology and by the Dipartimenti di Eccellenza 2023-2027, Legge 232/2016 project n. 40613, funded by the MUR).

Author contributions

G.R. performed the bioinformatics analysis. V.M. performed the drosophila experiments. A.VC. analyzed protein homology and performed structural modeling, molecular simulations, and AlphaFolding. M.P. performed the analysis of CEBPZ expression and contributed to the final version of the manuscript. G.B. analyzed and contributed to the drafting of the data expression in tumors. P.B. drafted the initial manuscript, conceived the study, participated in its design, coordinated and supervised the team, and edited the final manuscript. All authors have read and agreed to the published version of the manuscript.

Competing interest

No competing interests are declared.

Data availability statement

Data supporting the study for Figure 2 and Supplementary File 2 are available in DepMap [50] at the URL https://depmap.org/portal using the keywords:

CEBPZ, https://depmap.org/portal/gene/CEBPZ?tab=overview Top 100 co-dependencies.

NOC2L, https://depmap.org/portal/gene/NOC2L?tab=overview Top 100 co-dependencies.

NOC3L, https://depmap.org/portal/gene/NOC3L?tab=overview Top 100 co-dependencies.

DepMap, Broad (2024). DepMap 24Q4 Public. Figshare+. Dataset.

https://doi.org/10.25452/figshare.plus.24667905.v2 [49, 50]

Data supporting the study in Figures 3 and 4 are available from UALCAN [32, 33] at https://ualcan.path.uab.edu/openly. Using the keywords:

CEBPZ, NOC2L, and NOC3L at https://ualcan.path.uab.edu/cgi-bin/ualcan-res.pl. and then select the respective expression from the tumors from the list.

Gepia - GEPIA2 at http://gepia2.cancer-pku.cn/#index

using the keywords CEBPZ, NOC2L, and NOC3L.

Funding

This work was supported by a NIH Public Health Service grant from NIH-SC1DK085047 to PB and Pallotti Legacy for Cancer Research to MP. GR is a recipient of a fellowship PhD PON program 'Research and Innovation' 2014-2020 with financial support from REACT-EU resources.

Bibliography:

1. Vanden Broeck A, Klinge S. Eukaryotic Ribosome Assembly. Annu Rev Biochem 2024; 93:189-210.

2. Penzo M, Montanaro L, Trere D, Derenzini M. The Ribosome Biogenesis-Cancer Connection. Cells 2019; 8.

3. Dorner K, Ruggeri C, Zemp I, Kutay U. Ribosome biogenesis factors-from names to functions. EMBO J 2023; 42:e112699.

4. Hwang SP, Denicourt C. The impact of ribosome biogenesis in cancer: from proliferation to metastasis. NAR Cancer 2024; 6:zcae017.

5. Edskes HK, Ohtake Y, Wickner RB. Mak21p of Saccharomyces cerevisiae, a homolog of human CAATT-binding protein, is essential for 60 S ribosomal subunit biogenesis. J Biol Chem 1998; 273:28912-20.

6. Milkereit P, Gadal O, Podtelejnikov A, Trumtel S, Gas N, Petfalski E, et al. Maturation and intranuclear transport of pre-ribosomes requires Noc proteins. Cell 2001; 105:499-509.

7. Li N, Yuan L, Liu N, Shi D, Li X, Tang Z, et al. SLOW WALKER2, a NOC1/MAK21 homologue, is essential for coordinated cell cycle progression during female gametophyte development in Arabidopsis. Plant Physiol 2009; 151:1486-97.

8. Sanghai ZA, Piwowarczyk R, Broeck AV, Klinge S. A co-transcriptional ribosome assembly checkpoint controls nascent large ribosomal subunit maturation. Nat Struct Mol Biol 2023; 30:594-9.

9. Hurt E, Iwasa J, Beckmann R. SnapShot: Eukaryotic ribosome biogenesis II. Cell 2024; 187:1314- e1.

10. Vanden Broeck A, Klinge S. Principles of human pre-60S biogenesis. Science 2023; 381:eadh3892.

11. Destefanis F, Manara V, Santarelli S, Zola S, Brambilla M, Viola G, et al. Reduction of nucleolar NOC1 leads to the accumulation of pre-rRNAs and induces Xrp1, affecting growth and resulting in cell competition. J Cell Sci 2022; 135.

12. Manara V, Radoani M, Belli R, Peroni D, Destefanis F, Angheben L, et al. NOC1 is a direct MYC target, and its protein interactome dissects its activity in controlling nucleolar function. Front Cell Dev Biol 2023; 11:1293420.

13. Friedel RH, Seisenberger C, Kaloff C, Wurst W. EUCOMM--the European conditional mouse mutagenesis program. Brief Funct Genomic Proteomic 2007; 6:180-5.

14. Ciani Y, Fedrizzi T, Prandi D, Lorenzin F, Locallo A, Gasperini P, et al. Allele-specific genomic data elucidate the role of somatic gain and copy-number neutral loss of heterozygosity in cancer. Cell Syst 2022; 13:183-93 e7.

15. Lum LS, Sultzman LA, Kaufman RJ, Linzer DI, Wu BJ. A cloned human CCAAT-box-binding factor stimulates transcription from the human hsp70 promoter. Mol Cell Biol 1990; 10:6709-17.

16. Herold T, Metzeler KH, Vosberg S, Hartmann L, Rollig C, Stolzel F, et al. Isolated trisomy 13 defines a homogeneous AML subgroup with high frequency of mutations in spliceosome genes and poor prognosis. Blood 2014; 124:1304-11.

17. Yu L, Yin B, Qu K, Li J, Jin Q, Liu L, et al. Screening for susceptibility genes in hereditary non-polyposis colorectal cancer. Oncol Lett 2018; 15:9413-9.

18. Huang Y, Lin L, Shen Z, Li Y, Cao H, Peng L, et al. CEBPG promotes esophageal squamous cell carcinoma progression by enhancing PI3K-AKT signaling. Am J Cancer Res 2020; 10:3328-44.

19. Barbieri I, Tzelepis K, Pandolfini L, Shi J, Millan-Zambrano G, Robson SC, et al. Promoter-bound METTL3 maintains myeloid leukaemia by m(6)A-dependent translation control. Nature 2017; 552:126-31.

20. Li Y, Wang L, Liu X, Zhang C, Du X, Xing B. NIR promotes progression of colorectal cancer through regulating RB. Biochim Biophys Acta Mol Cell Res 2021; 1868:118856.

21. Ma CA, Pusso A, Wu L, Zhao Y, Hoffmann V, Notarangelo LD, et al. Novel INHAT repressor (NIR) is required for early lymphocyte development. Proc Natl Acad Sci U S A 2014; 111:13930-5.

22. Wu J, Zhang Y, Wang Y, Kong R, Hu L, Schuele R, et al. Transcriptional repressor NIR functions in the ribosome RNA processing of both 40S and 60S subunits. PLoS One 2012; 7:e31692.

23. Tominaga K, Johmura Y, Nishizuka M, Imagawa M. Fad24, a mammalian homolog of Noc3p, is a positive regulator in adipocyte differentiation. J Cell Sci 2004; 117:6217-26.

24. Yan C, Zhu M, Ding Y, Yang M, Wang M, Li G, et al. Meta-analysis of genome-wide association studies and functional assays decipher susceptibility genes for gastric cancer in Chinese populations. Gut 2020; 69:641-51.

25. Walters KB, Dodd ME, Mathias JR, Gallagher AJ, Bennin DA, Rhodes J, et al. Muscle degeneration and leukocyte infiltration caused by mutation of zebrafish Fad24. Dev Dyn 2009; 238:86-99.

26. Cheung MH, Amin A, Wu R, Qin Y, Zou L, Yu Z, Liang C. Human NOC3 is essential for DNA replication licensing in human cells. Cell Cycle 2019; 18:605-20.

27. Jumper J, Evans R, Pritzel A, Green T, Figurnov M, Ronneberger O, et al. Highly accurate protein structure prediction with AlphaFold. Nature 2021; 596:583-9.

28. Varadi M, Anyango S, Deshpande M, Nair S, Natassia C, Yordanova G, et al. AlphaFold Protein Structure Database: massively expanding the structural coverage of protein-sequence space with high-accuracy models. Nucleic Acids Res 2022; 50:D439-D44.

29. Meng EC, Goddard TD, Pettersen EF, Couch GS, Pearson ZJ, Morris JH, Ferrin TE. UCSF ChimeraX: Tools for structure building and analysis. Protein Sci 2023; 32:e4792.

30. Goddard TD, Huang CC, Meng EC, Pettersen EF, Couch GS, Morris JH, Ferrin TE. UCSF ChimeraX: Meeting modern challenges in visualization and analysis. Protein Sci 2018; 27:14-25.

31. UniProt C. UniProt: the Universal Protein Knowledgebase in 2025. Nucleic Acids Res 2024.

32. Chandrashekar DS, Karthikeyan SK, Korla PK, Patel H, Shovon AR, Athar M, et al. UALCAN: An update to the integrated cancer data analysis platform. Neoplasia 2022; 25:18-27.

33. Chandrashekar DS, Bashel B, Balasubramanya SAH, Creighton CJ, Ponce-Rodriguez I, Chakravarthi B, Varambally S. UALCAN: A Portal for Facilitating Tumor Subgroup Gene Expression and Survival Analyses. Neoplasia 2017; 19:649-58.

34. Cerami E, Gao J, Dogrusoz U, Gross BE, Sumer SO, Aksoy BA, et al. The cBio cancer genomics portal: an open platform for exploring multidimensional cancer genomics data. Cancer Discov 2012; 2:401-4.

35. Chaudhary KR, Kinslow CJ, Cheng H, Silva JM, Yu J, Wang TJ, et al. Smurf2 inhibition enhances chemotherapy and radiation sensitivity in non-small-cell lung cancer. Sci Rep 2022; 12:10140.

36. Penzo M, Guerrieri AN, Zacchini F, Trere D, Montanaro L. RNA Pseudouridylation in Physiology and Medicine: For Better and for Worse. Genes (Basel) 2017; 8.

37. Zhang X, Li W, Sun S, Liu Y. Advances in the structure and function of the nucleolar protein fibrillarin. Front Cell Dev Biol 2024; 12:1494631.

38. Marcel V, Ghayad SE, Belin S, Therizols G, Morel AP, Solano-Gonzalez E, et al. p53 acts as a safeguard of translational control by regulating fibrillarin and rRNA methylation in cancer. Cancer Cell 2013; 24:318-30.

39. Luo H, Kharas MG. Dotting Out AML by Targeting Fibrillarin. Cancer Res 2024; 84:2759-60.

40. Nguyen Van Long F, Lardy-Cleaud A, Carene D, Rossoni C, Catez F, Rollet P, et al. Low level of Fibrillarin, a ribosome biogenesis factor, is a new independent marker of poor outcome in breast cancer. BMC Cancer 2022; 22:526.

41. Zacchini F, Venturi G, De Sanctis V, Bertorelli R, Ceccarelli C, Santini D, et al. Human dyskerin binds to cytoplasmic H/ACA-box-containing transcripts affecting nuclear hormone receptor dependence. Genome Biol 2022; 23:177.

42. Alnafakh R, Saretzki G, Midgley A, Flynn J, Kamal AM, Dobson L, et al. Aberrant Dyskerin Expression Is Related to Proliferation and Poor Survival in Endometrial Cancer. Cancers (Basel) 2021; 13.

43. Kan G, Wang Z, Sheng C, Chen G, Yao C, Mao Y, Chen S. Dual Inhibition of DKC1 and MEK1/2 Synergistically Restrains the Growth of Colorectal Cancer Cells. Adv Sci (Weinh) 2021; 8:2004344.

44. Guerrieri AN, Zacchini F, Onofrillo C, Di Viggiano S, Penzo M, Ansuini A, et al. DKC1 Overexpression Induces a More Aggressive Cellular Behavior and Increases Intrinsic Ribosomal Activity in Immortalized Mammary Gland Cells. Cancers (Basel) 2020; 12.

45. Elsharawy KA, Mohammed OJ, Aleskandarany MA, Hyder A, El-Gammal HL, Abou-Dobara MI, et al. The nucleolar-related protein Dyskerin pseudouridine synthase 1 (DKC1) predicts poor prognosis in breast cancer. Br J Cancer 2020; 123:1543-52.

46. Stockert JA, Gupta A, Herzog B, Yadav SS, Tewari AK, Yadav KK. Predictive value of pseudouridine in prostate cancer. Am J Clin Exp Urol 2019; 7:262-72.

47. Tang Z, Kang B, Li C, Chen T, Zhang Z. GEPIA2: an enhanced web server for large-scale expression profiling and interactive analysis. Nucleic Acids Res 2019; 47:W556-W60.

48. Ge SX, Jung D, Yao R. ShinyGO: a graphical gene-set enrichment tool for animals and plants. Bioinformatics 2020; 36:2628-9.

49. Fong SH, Kuenzi BM, Mattson NM, Lee J, Sanchez K, Bojorquez-Gomez A, et al. A multilineage screen identifies actionable synthetic lethal interactions in human cancers. Nat Genet 2024.

50. Tsherniak A, Vazquez F, Montgomery PG, Weir BA, Kryukov G, Cowley GS, et al. Defining a Cancer Dependency Map. Cell 2017; 170:564-76 e16.

51. Meyers RM, Bryan JG, McFarland JM, Weir BA, Sizemore AE, Xu H, et al. Computational correction of copy number effect improves specificity of CRISPR-Cas9 essentiality screens in cancer cells. Nat Genet 2017; 49:1779-84.

52. Dempster JM, Boyle I, Vazquez F, Root DE, Boehm JS, Hahn WC, et al. Chronos: a cell population dynamics model of CRISPR experiments that improves inference of gene fitness effects. Genome Biol 2021; 22:343.